Proceedings World Geothermal Congress 2015
Melbourne, Australia, 19-25 April 2015

Semi-Analytical Temperature and Stress Profiles for Nonisothermal CO2 Injection

Tara LaForce[1,2], Bisheng Wu[2], Jonathan Ennis-King[1,2], Lincoln Paterson[1,2]

[1]CO2CRC, [2]CSIRO, Energy, Private Bag 10, Clayton South, VIC 3169, Australia

tara.laforce@csiro.au

Keywords: method of characteristics, CO_2, near-well stress, nonisothermal injection, thermal fracturing

ABSTRACT

Reservoir cooling at the injection interval is expected if CO_2 is used as a heat carrier fluid in multi-well enhanced geothermal systems. Cooling the reservoir near the well alters the stress field. The tensile fracture pressure is reduced at the injection well perforations when the temperature difference between injected fluid and the reservoir is large.

In this work semi-analytical models are used to estimate the relative length-scales and magnitude of thermal, saturation, pressure and stress distributions for constant rate, nonisothermal CO_2 injection into a porous medium that is initially water saturated. Advection-dominated radial flow is assumed so that the coupled two-phase flow and thermal conservation laws can be solved analytically. The resulting saturation and thermal profiles are then used in semi-analytical estimates of the pore pressure and *in situ* stress changes in the reservoir.

1. INTRODUCTION

There has been considerable discussion in the literature about potentially using carbon dioxide (CO_2) as a heat carrier fluid for enhanced geothermal energy systems (EGS) (for example, see Brown, 2000; Pruess 2006, 2008; Atrens et al, 2008; Spycher and Pruess, 2010; Randolph and Saar, 2011; Remoroza et al, 2012; Vilarrasa et al, 2014). The concept was originally introduced by Brown (2000), who proposed injection of CO_2 into a confined, dry geothermal reservoir as potentially preferable to water injection. Supercritical CO_2 may have improved thermodynamic and flow properties compared to water because of the low viscosity of CO_2 at high temperatures and pressures. Remoroza et al (2012) demonstrated that dry CO_2 is unlikely to have geochemical interactions with prospective EGS reservoirs. Moreover CO_2 has a substantial increase in density with decreasing temperature, which reduces re-injection costs (Pruess, 2006; Atrens et al, 2008). Finally, loss of CO_2 into the target formation may allow for storage of large quantities of CO_2, making the EGS system a carbon-negative source of energy.

One disadvantage of using CO_2 as a carrier fluid is the substantial start-up cost and time in CO_2 EGS. Most target formations for EGS will initially be water-saturated and the resident water must be removed from the reservoir by injection of CO_2 and removal of water through injector-producer well pairs (for example, see Spycher and Pruess, 2010). During the early stage of two-phase flow the pressure build-up near the injection well may be substantial and result in fracturing of the reservoir. Injection of substantially colder fluid, which is most likely to be the case, may increase the likelihood of reservoir fracturing. Depending on the engineering constraints of the particular EGS system, fracturing may be desirable because it will increase in permeability, or undesirable because uncontrolled fracturing could cause loss or leakage of fluids.

Long-term temperature changes due to CO_2 injection have been observed in the CO2CRC Otway CO_2 storage demonstration project and similar near-well temperature changes are expected in CO_2 EGS. Vilarrasa et al (2014) studied the impact of cold CO_2 injection on the cap-rock and reservoir integrity in CO_2 storage. Numerical simulations were run for both vertical and horizontal wells, as well as normal and reverse faulting stress regimes. Overall the results were very positive, with little likelihood of cap-rock failure for realistic injection rates and rock properties.

In previous works (LaForce et al 2014a, 2014b), the authors have considered the impact of nonisothermal immiscible fluid injection on reservoir pressure and stress in the context of CO_2 and natural gas storage sedimentary basins. In the present work the models developed in LaForce et al (2014a, 2014b) are briefly introduced. An example problem is outlined which is representative of an injection scenario for CO_2 EGS in a fractured granite which is relatively shallow but has high temperature. Solutions to the example problem are presented. Finally the implications of the results for CO_2 EGS are discussed, along with limitations of the semi-analytical model.

2. MATHEMATICAL MODEL

A schematic of the flow problem is shown in Figure 1. The mathematical model in this work is based on the assumption of purely radial flow of fluids and energy, coupled with vertical diffusion of energy. The solution to these conservation laws are then forward coupled to an approximate model for the radial pressure increase in the reservoir. Finally the pressure and thermal profiles are used in an analytical approximation to the radial displacement of the reservoir, which gives the radial and tangential stress within the injection formation.

2.1 Saturation and Temperature

The conservation laws for radial purely-advective flow of water in the presence of immiscible CO_2 is given by Eq. 1. The over and underburden formations are assumed to be completely impermeable so there is no vertical flow. The energy equation is also formulated as a conservation law with independent variable temperature, T. Temperature is assumed to change radially purely by advection with the injected fluid and vertically by diffusion only, as given by Eq. 2. The conservation laws for fluid and energy are:

$$\frac{\partial S_1}{\partial t_D} + \frac{\partial f_1}{\partial x_D} = 0 \tag{1}$$

$$\frac{\partial T_D}{\partial t_D} + \frac{f_1 + \alpha}{S_1 + \beta}\frac{\partial T_D}{\partial x_D} = \frac{-\gamma U T_D}{S_1 + \beta} \tag{2}$$

where S_1, and f_1 are dimensionless saturation and fractional flow of the water phase. $T_D = (T-T_i)/(T_w-T_i)$ is the normalized temperature where T_i is the initial temperature and T_w is the injection temperature at the well. The dimensionless radius is $x_D = r^2/L^2$ and dimensionless time is $t_D = qt/(\pi\phi_r L^2 h)$ where r is radial distance from the well, L is radius of the reservoir, q is volumetric injection rate, t is time, ϕ_r is porosity of the reservoir and h is the height of the reservoir. The heat-loss term U and the conductivity parameters of the reservoir are given by:

$$\alpha = \frac{\rho_2 C_2}{\rho_1 C_1 - \rho_2 C_2} \qquad \beta = \frac{\rho_2 C_2 + \frac{1-\phi_r}{\phi_r}\rho_s C_s}{\rho_1 C_1 - \rho_2 C_2}$$
$$\gamma = \frac{L^2 \pi}{q(\rho_1 C_1 - \rho_2 C_2)} \qquad U = \sqrt{\frac{qK_a(\rho C)_a}{t_D \pi \phi_r L^2 h}} \tag{3}$$

where ρ_j is the density of phase j for the liquid (j=1), gas (j=2) or the solid (j=s), C_j is the mass-based heat capacity of phase j, K_a is the saturated thermal conductivity of the adjacent formations, and $(\rho C)_a$ are the density and heat capacity of the over and under-burden formations. The water-saturated over and underburden must have the same rock and thermal properties for vertical symmetry in the mathematical model, but these properties may be different than the properties of the reservoir. The heat-loss term is based on the model proposed by Lauwerier (1955). The solutions to Eqs. 1-2 with U = 0 are derived in Sumnu-Dindoruk and Dindoruk (2008). A full derivation and discussion of the solutions to the coupled conservation laws is given in LaForce et al (2014a) and is not repeated here.

As written in Eq. 2, the temperature along the characteristic must be numerically integrated. However, it was shown in LaForce et al (2014b) that it is possible to obtain an approximate solution to the thermal equation by using the average flux f_1 behind the thermal front. This approximation will be used in the current work.

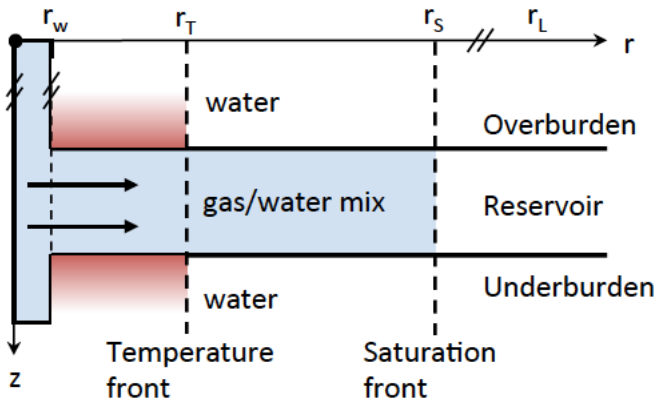

Figure 1: Schematic of flow in the reservoir as idealized for the semi-analytical model. CO_2 flows radially outward from the well. Thermal energy advects radially within the reservoir and diffuses vertically into the under and overburden formations (Reprinted from Advances in Water Resources, LaForce, T., Ennis-King, J. and Paterson, L., Analytical solutions for nonisothermal injection including heat loss from the reservoir, part 1: Saturation and temperature, (2014), with permission from Elsevier.).

2.2 Pressure in the Reservoir

As shown in Mijić et al (2014), at any given time, t_D^*, the pressure in the reservoir is:

$$\left.\frac{dP}{dx_D}\right|_{t_D^*} = \frac{q}{4\pi k h x_D}\frac{1}{M} \tag{4}$$

where M is the overall mobility of the fluid or fluid mixture, k is the absolute permeability of the reservoir and P is the pressure. The pressure equation can be solved with either an open outer boundary (infinite reservoir) or a fixed pressure outer-boundary. Only the open boundary will be considered here.

For the single-phase part of the solution, ahead of the injected CO_2 front, the transient model from Dake (1978) is the correct solution to Eq. 4. Mijić et al (2014) proposed to approximate the solution to Eq. 4 by numerically integrating the profile in the two-phase region. Aziz and Cinar (2013) proposed a second way of approximating the solution to Eq. 4 by using average mobilities in the two-phase region. For suitably large times, and/or small radii, the exponential integrals in the Azizi and Cinar approximation can be reduced to a series of natural logs, which allows for a closed-form analytical solution for the pressure. It was shown in LaForce et al (2014b) that the small argument (small radius, or large time) approximation to the Azizi and Cinar (2013) model was sufficiently accurate to use in generating stress profiles in the reservoir for the example examined in that work. However, the pressure build-up in that example was small, so it remains to be seen whether this is a general result. Both models will be examined here.

2.3 Stress in the Reservoir

As shown in LaForce et al (2014b), the model of Rehbinder (1995) can be adapted to the thermal and pressure profiles developed in the preceding sections. The radial displacement, u, of the reservoir rock is given by (Rehbinder, 1995):

$$\frac{d}{d\xi}\left(\frac{1}{\xi}\frac{d}{d\xi}(\xi u_D)\right)\Bigg|_{t_D^*} = \frac{dT_{D2}}{d\xi} + \left(\frac{1-2\upsilon}{1-\upsilon}\right)\frac{dP_D}{d\xi} \tag{5}$$

where $u_D = u(1-\nu)/[\alpha_B T_r r_w (1+\nu)]$, r_w is the radius of the wellbore and $T_r = T_i - T_w$ is the relative temperature. $\xi = r/r_w$ is a new dimensionless radius and $T_{D2} = T_D$ if $T_w > T_i$ and $T_{D2} = -T_D$ if $T_w < T_i$ is the new dimensionless temperature. Dimensionless pressure is given by $P_D = (P-P_o)(1-\nu)/(\alpha_B T_r E)$ for initial pore pressure P_o. The rock properties ν, E and α_B are the drained Poission ratio, drained Young's modulus and Biot pore-pressure coefficient, respectively. Solutions for the effective radial and tangential stresses in the reservoir are then generated from the displacement of the solid.

Using the analytical approximation to the pressure in the reservoir, P_D, along with the approximation to the thermal profile, T_D, it is possible to develop a closed-form analytical solution for the radial displacement of the porous medium, radial, and tangential stresses with zero capillary pressure from Eq. 5. If it is necessary to use the numerically-integrated pressure profile, then the solution to Eq. 5 also contains a numerical integral (LaForce et al, 2014b).

The Rehbinder model must be solved on a finite domain of length L. Solutions have been derived for constant stress or zero displacement outer boundaries. In LaForce et al (2014b) the outer boundary condition was shown to have a relatively minor impact on the stress in the reservoir for the example problem, so only the zero displacement outer boundary condition will be considered in the present work.

3. RESULTS IN AN EXAMPLE GEOTHERMAL SYSTEM

Table 1 shows the parameters used in the example solutions. These are chosen to be representative of CO_2 injection into a normally-pressured granite formation with depth of 2 km. At the reservoir conditions CO_2 will be a supercritical fluid.

The initial vertical stress, σ_v, is computed assuming an average overburden density of 2700 kg/m^3 and the initial horizontal stress is calculated from $\sigma_h = \sigma_v \nu/(1-\nu)$. Assuming a typical fracture pressure gradient of 15.8 kPa/m (0.7 psi/ft), the compressive fracture pressure of this formation would be 31.6 MPa, which is 11.6 MPa more compressive than the initial reservoir pressure. The tensile fracture pressure is estimated from the correlation in Wu et al (2010) to be 7.12 MPa.

The formation is assumed to have very high temperature for this depth, T = 200 ^{o}C, as would be necessary to make EGS feasible. Granite naturally has a very low porosity and permeability so it is assumed that the formation has been fractured and the fracture network dominates flow. To represent a well-connected fracture network, low exponents n = 1.5 and relatively low residual saturations are chosen for the Corey-type relative permeability parameters. Corey exponents of one with zero residuals would represent flow through completely open fractures.

3.1 Saturation and Temperature

Figure 2 shows the saturation and temperature profiles for the example problem outlined in Table 1. Eqs. 1-2 are solved as discussed in detail in LaForce et al (2014a, 2014b). The numerically-integrated solution to the thermal equation for this example was also found, and the resulting temperature profile was indistinguishable from the analytical solution using the average flux.

Radial distance is shown on Figure 2 on a log scale to emphasize the near-well region. In this example the saturation front moves into the reservoir an order of magnitude more quickly than the thermal front, which is extremely slow moving. After five years of injection the thermal front has only penetrated 200 m from the well, while the saturation front has traveled 2.5 km. The order of magnitude difference in velocities is largely due to the low porosity, ϕ_r = 5%, of the injection formation. The small amount of pore-space available for flow means that the injected CO_2 moves quickly outwards from the well. Conversely, the formation is 95% granite, which has a much higher heat capacity than the injected CO_2; the rock must be heated until a local equilibrium temperature is reached everywhere behind the thermal front, which substantially delays the thermal front as compared with a higher porosity formation.

3.2 Pressure in the Reservoir

The exact and simplified solutions to the pressure model in Eq. 3 are shown at the top of Figure 3 for the parameters outlined in Table 1. The top subfigure shows a direct comparison of the simplified and numerically integrated models after one hour and five years. As can be seen, the approximate solution captures the pressure profile away from the well, but substantially underestimates the pressure in the first meter of the reservoir. The bottom subfigure shows the approximate pressure solution at four times. Each of the profiles is truncated at the radius where the approximate pressure solution becomes invalid (Dake, 1978).

Table 1 Fluid and reservoir parameters for the example problem. Rock and relative permeability parameters are chosen to be representative of fractured granite.

Injection time (yr)	5	Reservoir porosity, ϕ_r, (-)	0.05
CO_2 injection rate (million metric tonne/yr)	0.5	Reservoir rock heat capacity, C_r, (kJ/kg K)	0.79
Injection fluid temperature, T_w, (^{o}C)	20	Reservoir rock density, ρ_r, (kg/m^3)	2700.0
Initial reservoir temperature, T_i, (^{o}C)	200	Adjacent formation porosity, ϕ_a, (-)	0.005
Initial reservoir pressure, P_o, (MPa)	20	Adjacent formation heat capacity, C_a, (kJ/kg K)	0.83
Reservoir thickness, h, (m)	10	Adjacent formation rock density, ρ_a, (kg/m^3)	2800.0
Reservoir radius, L, (km)	10	Corey exponent, n, (-)	1.5
Wellbore radius, r_w, (m)	0.1	Water and gas phase residuals, S_{jr}, (-)	0.2, 0.205
Absolute permeability, k, (mD)	50	Thermal expansion coefficient, α_B, (-)	5×10^{-6}
Young's modulus, E, (MPa)	40×10^3	Biot coefficient, B_i, (-)	0.72
Poisson's ratio, ν (-)	0.2	Fluid compressibility, c, (Pa^{-1})	4.4×10^{-10}
Initial horizontal stress, σ_h, (MPa)	-13.5	Initial vertical stress, σ_v, (MPa)	-54.0
Compressive fracture pressure, P_f, (MPa)	-31.6	Tensile fracture pressure, P_f, (MPa)	7.12
Effective tensile strength of the reservoir, σ_T, (MPa)	10.0		

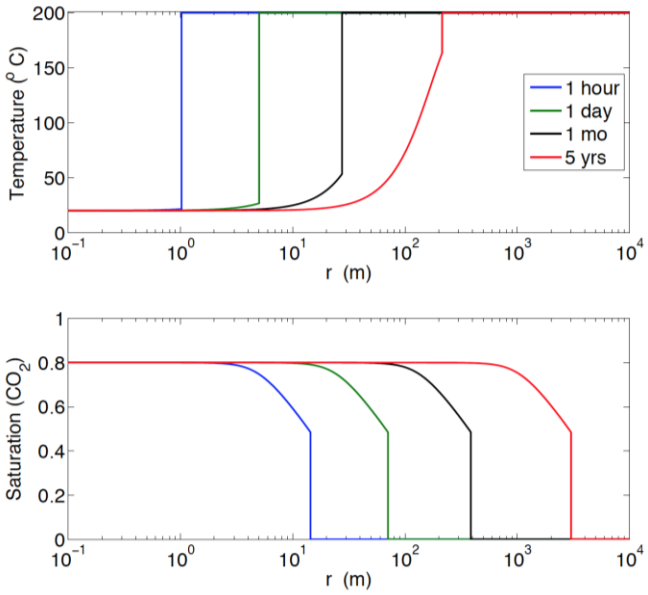

Figure 2: Saturation and temperature in the reservoir vs log of the radius from the well. Temperature profiles are from the approximate analytical solution for the times indicated. The thermal front moves approximately an order of magnitude more slowly than the saturation front.

As can be seen in Figure 3, for the injection rate and permeability of the reservoir the injection pressure quickly becomes very high in the first meter of the reservoir. At the end of five years of injection the increase in pressure at the well is 21.5 MPa. The total reservoir pressure at the well is 41.5 MPa, more than double the initial reservoir pressure of 20 MPa and well above the estimated compressive fracture pressure of this formation of 31.6 MPa. Thus the injection rate used in this example could only be sustained if the first few meters of the well were fractured to increase permeability prior to the start of CO_2 injection.

All coupling in this work is one-way, and so there is no feedback between the increased pressure and the properties of the fluids. Mijić et al (2014) presented an iterative method wherein the average pressure of the two-phase region was used to update water and CO_2 properties for a model that included Forchheimer flow of the gas phase and partitioning of the components between the water,

gas and solid salt phases. Using this iterative method, Mijić et al (2014) were able to benchmark their solutions against a commercial simulator. In order to test the impact of increasing pressure on the displacement in the current work, the solution was found for the parameters in Table 1 and an average reservoir pressure of 30 MPa, slightly higher than the radially-averaged pressure in the two-phase region after 5 years of injection. Unexpectedly, after five years of injection the high-pressure solution showed a smaller injection pressure increase at the well by about 4 MPa. Though the fluid viscosities increased, substantially higher CO_2 density at 30 MPa caused the volumetric injection rate q to decrease, which resulted in lower injection pressure. The thermal front moved slightly faster at high pressure, increasing from a dimensionless velocity of 0.0083 to 0.011, while the leading saturation shock velocity increased from a dimensionless velocity of 1.59 to 1.64. Overall, ignoring the impact of increasing pressure on the fluid viscosities and densities appears to have relatively little impact on the saturation and thermal profiles in the example problem.

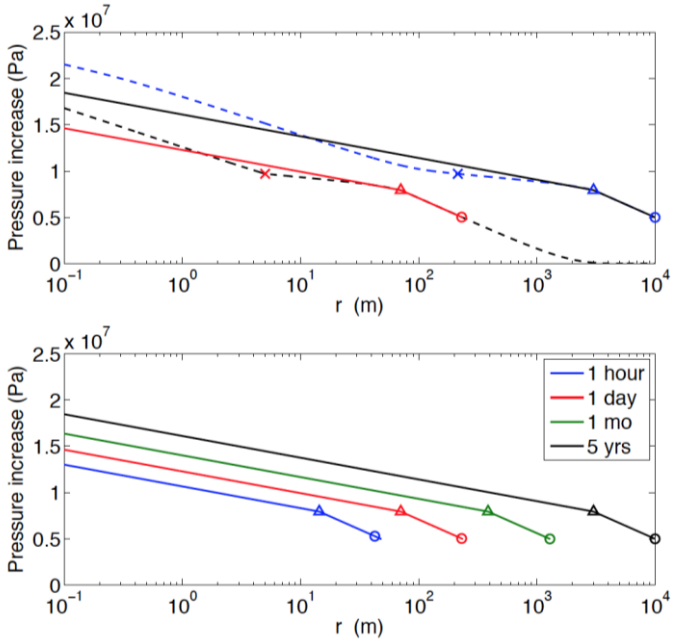

Figure 3: Pressure increase in the reservoir as a function of radial distance. Top: Comparison of the simplified and numerically integrated models after one day and five years of injection. Analytical solutions are shown as solid lines: red (one day), black (five years). Numerically integrated models are shown as dashed lines: black (one day) blue (five years). The triangles indicate the end of the two-phase region, 'x's indicate the location of the thermal shock, and circles indicate the maximum radius at which the approximate analytical solution is valid. Bottom: simplified pressure profiles at the four times indicated. Solutions are truncated at the radius where the simplified model is no longer valid.

3.3 Stress in the reservoir

Finally the stress in the reservoir is found for the example problem outlined in Table 1. As the match between the analytical and numerical pressure profiles is not very good near the well, the stress field is found for both the numerically integrated temperature/pressure models and the analytical approximations to the temperature and pressure. As can be seen in Figure 4, everywhere in the reservoir the radial and tangential stresses are extremely similar, indicating that the analytical solution is a sufficient approximation of the pressure for the purposes of computing stress in the reservoir.

The temperature, displacement, radial and tangential stresses at four injection times are shown in Figure 5. As can be seen, negative displacement of the formation occurs behind the thermal front, which causes the formation to go into tension near the well. At later time the change in temperature across the thermal shock decreases which result in the change in stress also decreasing. The displacement becomes more compressive at later time due to increasing pressure throughout the reservoir, as shown in Figure 3.

After one day of injection the tangential stress exceeds the tensile fracture pressure from the well to just behind the thermal front, around one meter into the reservoir. At that time the radial stress also exceeds the tensile fracture pressure for a few centimeters behind the thermal front. The tangential stress in the first few centimeters of the reservoir exceeds the tensile fracture pressure and the radial stress exceeds compressive fracture pressure for the duration of CO_2 injection.

The isothermal stress fields (not shown) were also found by setting $T_D = 0$ in Eq. 5. When the impact of temperature is not taken into account, injection overpressure causes radial stresses in excess of the compressive fracture pressure. Fracture pressures are not exceeded anywhere else in the reservoir.

4. DISCUSSION

In this example problem the relevant length-scales for the coupled flow and stress problem ranges from very high tangential stresses just a few centimeters from the well to pressure build up at the reservoir boundary, 10 km from the well. By using an analytical model it is simple to find the solution at any radius or time. The closed-form analytical solution for the reservoir stress,

approximate temperature, and approximate pressure allows for computation of any of the three without the need for iterative computations, once the average water flux and two-phase mobility have been computed.

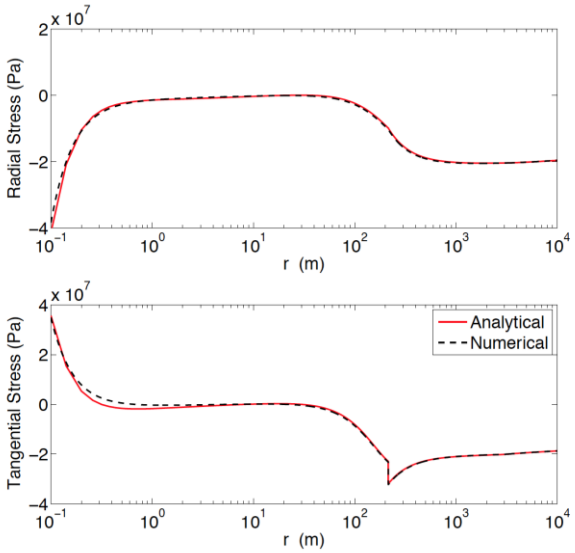

Figure 4: Comparison of stress in the reservoir after five years for the analytical (red) and numerically integrated (black) pressure and temperature approximations. Compressive stresses are shown as negative, while tensile stress is positive.

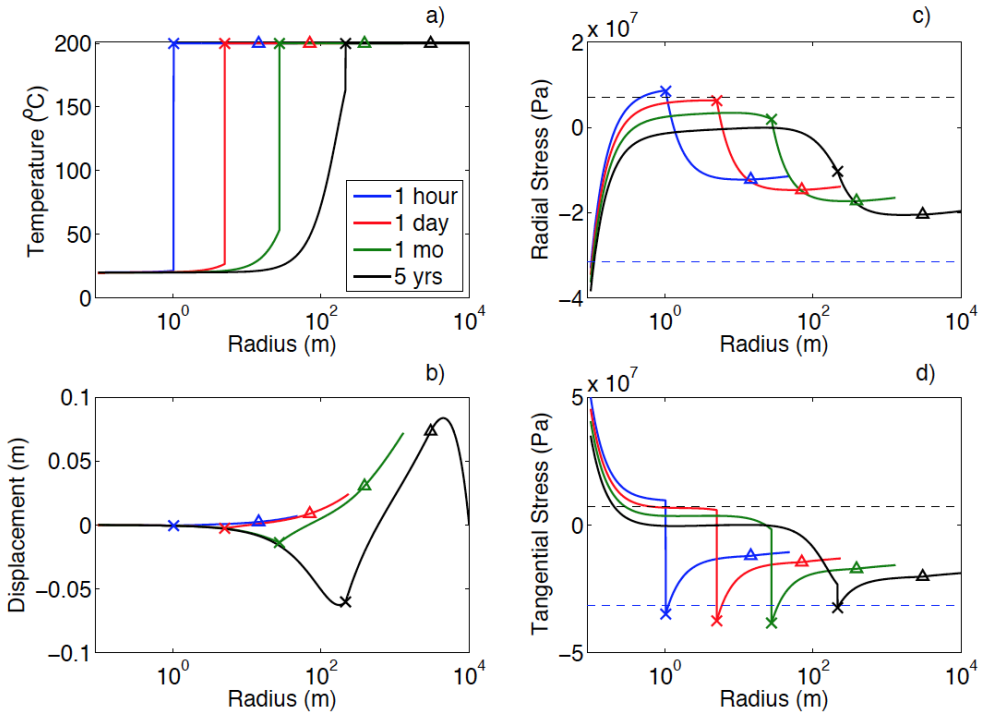

Figure 5: a) Temperature, b) displacement of the formation, c) radial and d) tangential stresses in the reservoir at four times. The black dashed line on the stress profiles indicates the tensile fracture pressure of 7.1 MPa, while the blue dashed line indicates the compressive fracture pressure of -31.6 MPa. Compressive stresses are shown as negative, while tensile stress is positive. The triangles indicate the end of the two-phase region and 'x's indicate the location of the thermal shock. The profiles terminate at the radius where the approximation for the pressure profile is no longer valid.

The low temperature region caused by cold CO_2 injection propagates very slowly into the reservoir due to the low porosity and high rock volume of the granite formation. At the end of five years of injection the thermal front has only traveled about 200 m into the reservoir. This sharp and slowly moving thermal front causes tensile tangential stress near the well that is in excess of the tensile fracture pressure of the rock at early injection time. The radial stress is also above the tensile fracture pressure just behind the

thermal front. At later time only the tangential stress is in excess of the tensile fracture pressure, and only in the one meter nearest the well.

The tangential stress is highly compressive immediately ahead of the thermal front. At early and intermediate times the tangential stress changes across the shock front from near the tensile fracture pressure to below the compressive fracture pressure of the formation. This sudden change in stress state could cause fracturing away from the wellbore.

As the example problem had a low porosity and permeability, the injection pressure and resulting compressive radial stress at the well were unrealistically large. The first few meters of the well would need to be fractured to inject 0.5 million tonnes/year in this formation. Perforating the well after completion would solve this problem and is common practice in industry. The pressure perturbation reached the outer edge of the reservoir, 10 km from the well, within one month of injection. The displacement of the reservoir rock also becomes large near the outer boundary of the reservoir, but this had relatively little impact on the *in situ* stresses.

4.1 Limitations of the Analytical Models

Partitioning of the water and CO_2 between the liquid and gas phases has been left out of the solutions in this work. This will cause a small error in the saturation near the injection well, as the water fraction evaporated into the CO_2 phase is on the order of 0.0006 by volume at 20 ^oC. The small change in saturation may cause a large error in the pressure at the well because there is no evaporation of the residually trapped CO_2 (Azizi and Cinar, 2013). Ignoring component partitioning between the liquid and gas phases will also cause a small error in the velocity and saturation at the leading CO_2 front; however this difference may not be large as the mass fraction of CO_2 in the water phase at 200^oC is also approximately 0.0006 by volume (Spycher and Pruess, 2010). It is unclear how much ignoring phase partitioning impacts the thermal shock between the injection and initial temperatures.

Another limitation of the analytical model is the assumption that thermal energy is transported radially into the reservoir primarily by advection. The dimensionless velocity of the thermal shock is nearly constant, but in real distance the thermal shock slows down because $x_D = r^2/L^2$. Thus, the assumption of radial advection is a good approximation at short time, when the dimensional thermal front is moving quickly, but at later times the thermal diffusion will become increasingly important.

There is no feedback between the increasing stress, decreasing temperature and the porosity of the formation. As shown in the section on pressure, computation of a solution at higher pressure indicated that ignoring the feedback between pressure and fluid viscosity and density is not likely to result in a large error in the solution.

The overall impact of neglecting the impact of thermal stress on the porosity and permeability in the current work is unclear. At the well porosity will increase due to being under tension, which would result in lower injection pressure. However a few meters from the well the formation is under increasing compression due to the fluid injection, which would tend to decrease porosity and increase injection pressure.

Vilarrasa et al. (2014) included thermal effects on the porosity of the rocks in their simulations of cold CO_2 injection for storage. Their results showed that that it was important to include the thermal expansion of the solid in order to have the correct horizontal stress in the cooled region of the cap-rock above the well, but that the temperature-induced change in porosity was not significant in the reservoir. The case studied in the present work is a fracture-dominated reservoir with porosity and permeability that are higher than the cap-rock and lower than the reservoir studied in Vilarrasa et al (2014), so it is unclear whether the reservoir porosity and permeability will be sensitive to thermal or pressure changes. A simulation with two-way coupling and explicit fracture modeling would be necessary to study the impact of ignoring volumetric changes on reservoir stress.

4.2 Future Work

In the future it would be useful to include the impact of the water and CO_2 partitioning between the liquid and gas phases in the saturation and pressure equations. Azizi and Cinar (2013) showed that ignoring the evaporation of water near the injection well resulted in overestimating the near-well pressure in CO_2 storage. A study of the combinations of rock and fluid parameters that make tensile or compressive fracturing likely in nonisothermal injection would also be extremely useful. Finally it would be interesting to see how nonisothermal fluid injection impacts reservoir stress in other applications such as water or gas flooding for enhanced oil recovery.

5. CONCLUSIONS

Semi-analytical solutions for saturation, temperature, pressure and stress profiles presented in this paper demonstrate the impact of nonisothermal injection of CO_2 in a hypothetical enhanced geothermal energy project in a fractured granite reservoir. In initial screening of potential EGS sites very little will be known about the target formation properties and simplified solutions such as these can be used to quickly generate order-of-magnitude estimates on the area impacted by the injection of cold CO_2.

For the low porosity and permeability target formation, ignoring the impact of temperature on the reservoir stresses would result in a substantial underestimate of the potential for fracturing the reservoir. Thermally induced stresses may cause tensile failure due to radial stress or compressive failure due to tangential stress near the thermal front. The thermal perturbation and resulting thermal stresses propagate slowly into the reservoir, so any fracturing would occur within a few hundred meters of the well.

ACKNOWLEDGEMENTS

The authors acknowledge the funding provided by the Australian government through its CRC program to support this research.

REFERENCES

Atrens, A. D., Gurgenci, H., and Rudolph, V.: CO_2 thermosiphon for competitive geothermal power generation, *Energy and Fuels*, **23**, (2008), 553-557.

Azizi, E. and Cinar Y.: Approximate analytical solutions for CO_2 injectivity into saline formations. *SPE Reservoir Engineering and Evaluation*, **16**, (2013), 123-133.

Dake, L.P.: *Fundamentals of Reservoir Engineering*, volume 8 of *Developments in Petroleum Science*, Elsevier, (1978).

LaForce, T., Ennis-King, J. and Paterson, L.: Analytical solutions for nonisothermal injection including heat loss from the reservoir, part 1: Saturation and temperature, *Advances in Water Resources*, (2014a), 10.1016/j.advwatres.2014.08.008, *to appear*.

LaForce, T., Mijić, A., Ennis-King, J. and Paterson, L.: Analytical solutions for nonisothermal injection including heat loss from the reservoir, part 2: Pressure and stress, *Advances in Water Resources*, (2014b), 10.1016/j.advwatres.2014.08.008, *to appear*.

Lauwerier, H.A.: The transport of heat in an oil layer caused by the injection of hot fluid, *Applied Scientific Research, Section A*, **5**, (1955), 145-150.

Mijić, A., LaForce, T.C., and Muggeridge, A.H.: CO_2 injection in saline aquifers under non-Darcy conditions, *Water Resources Research*, **50**, (2014), DOI: 10.1002/2013WR014893.

Pruess, K.: Enhanced geothermal systems (EGS) using CO_2 as working fluid—A novel approach for generating renewable energy with simultaneous sequestration of carbon, *Geothermics,* **35**, (2006), 351-367.

Pruess, K.: On production behavior of enhanced geothermal systems with CO_2 as working fluid, *Energy Conversion and Management,* **49**, (2008), 1446-1454.

Randolph, J.B., and Saar, M.O.: Coupling carbon dioxide sequestration with geothermal energy capture in naturally permeable, porous geologic formations: Implications for CO_2 sequestration, *Energy Procedia,* **4**, (2011), 2206-2213.

Rehbinder. G.: Analytical solutions of stationary coupled therm-hydro-mechanical problems, *International Journal of Rock Mechanics*, **32**, (1995), 453-463.

Remoroza, A., Doroodchi, E., and Moghtaderi, B.: CO_2 EGS in hot dry rock: Preliminary results from CO_2-rock interaction experiments, *Proceedings*, 37th Workshop on Geothermal Reservoir Engineering, Stanford University, Stanford, CA, USA (2012).

Spycher, N. and Pruess, K.: A phase-partitioning model for CO_2–brine mixtures at elevated temperatures and pressures: Application to CO_2-enhanced geothermal systems, *Transport in Porous Media*, **82**, (2010), 173-196.

Sumnu-Dindoruk, D. and Dindoruk, B.: Analytical solution of nonisothermal Buckley-Leverett flow including tracers, *SPE Reservoir Engineering and Evaluation*, **11**, (2008), 555-564.

Vilarrasa, V., Olivella, S., Carrera, J. and Rutqvist, J.: Long term impacts of cold CO_2 injection on the caprock integrity, *International Journal of Greenhouse Gas Control,* **24**, (2014), 1-13.

Wahanik, H., Eftekhari, A.A., Bruining, J., Marchesin, D. and Wolf, K.H.: Analytical solutions for mixed CO_2-water injection in geothermal reservoirs, *Proceedings*, CSUG/SPE Canadian Unconventional Resources and International Petroleum Conference, Calgary, Alberta, Canada, (2010), CSUG/SPE 138154.

Wu, B., Zhang, X. and Jeffrey, R.G.: A thermo-poro-elastic analysis of stress fields around a borehole, *Proceedings*, ARMA 44th US Rock Mechanics Symposium and 5th US-Canada Rock Mechanics Symposium, Salt Lake City, UT, USA, (2010), ARMA 10-442.

Zhu, J., Jessen, K. and Orr, Jr., F.M.: Analytical solution for gas/oil displacement with temperature variation, *Proceedings*, SPE/DOE 14th Symposium on Improved Oil Recovery, Tulsa, Oklahoma, USA, (2004), SPE 89432.